

## Comparative metabolomics approach coupled with cell- and gene-based assays for species classification and anti-inflammatory bioactivity validation of *Echinacea* plants<sup>☆</sup>

Chia-Chung Hou<sup>a</sup>, Chun-Houh Chen<sup>b</sup>, Ning-Sun Yang<sup>a</sup>, Yi-Ping Chen<sup>a</sup>, Chiu-Ping Lo<sup>a</sup>, Sheng-Yang Wang<sup>c</sup>, Yin-Jing Tien<sup>d</sup>, Pi-Wen Tsai<sup>a</sup>, Lie-Fen Shyur<sup>a,e,\*</sup>

<sup>a</sup>Agricultural Biotechnology Research Center, Academia Sinica, Taipei 115, Taiwan, ROC

<sup>b</sup>Institute of Statistical Sciences, Academia Sinica, Taipei 115, Taiwan, ROC

<sup>c</sup>Department of Forestry, National Chung-Hsing University, Taichung 402, Taiwan, ROC

<sup>d</sup>Institute of Statistics, National Central University, Taoyuan County 320, Taiwan, ROC

<sup>e</sup>Department of Biochemical Science and Technology, National Taiwan University, Taipei 106, Taiwan, ROC

Received 26 March 2009; received in revised form 7 August 2009; accepted 26 August 2009

### Abstract

*Echinacea* preparations were the top-selling herbal supplements or medicines in the past decade; however, there is still frequent misidentification or substitution of the *Echinacea* plant species in the commercial *Echinacea* products with not well chemically defined compositions in a specific preparation. In this report, a comparative metabolomics study, integrating supercritical fluid extraction, gas chromatography/mass spectrometry and data mining, demonstrates that the three most used medicinal *Echinacea* species, *Echinacea purpurea*, *E. pallida*, and *E. angustifolia*, can be easily classified by the distribution and relative content of metabolites. A mitogen-induced murine skin inflammation study suggested that alkamides were the active anti-inflammatory components present in *Echinacea* plants. Mixed alkamides and the major component, dodeca-2*E*,4*E*,8*Z*,10*Z*(*E*)-tetraenoic acid isobutylamides (**8/9**), were then isolated from *E. purpurea* root extracts for further bioactivity elucidation. In macrophages, the alkamides significantly inhibited cyclooxygenase 2 (COX-2) activity and the lipopolysaccharide-induced expression of COX-2, inducible nitric oxide synthase and specific cytokines or chemokines [i.e., TNF- $\alpha$ , interleukin (IL)-1 $\alpha$ , IL-6, MCP-1, MIP-1 $\beta$ ] but elevated heme oxygenase-1 protein expression. Cichoric acid, however, exhibited little or no effect. The results of high-performance liquid chromatography/electron spray ionization/mass spectrometry metabolite profiling of alkamides and phenolic compounds in *E. purpurea* roots showed that specific phytochemical (i.e., alkamides, cichoric acid and rutin) contents were subject to change under certain post-harvest or abiotic treatment. This study provides new insight in using the emerging metabolomics approach coupled with bioactivity assays for medicinal/nutritional plant species classification, quality control and the identification of novel botanical agents for inflammatory disorders.

© 2010 Elsevier Inc. All rights reserved.

**Keywords:** *Echinacea*; Anti-inflammation; Metabolomics; Alkamides

### 1. Introduction

Metabolomics is one of the more-recently introduced “-omics” technologies, joining genomics, transcriptomics and proteomics as tools in global systems biology [1,2]. Metabolomics refers to the high-throughput analysis, either by a targeted or a global (unbiased) strategy, of the metabolic state of a biological system based on the simultaneous measurement of the distribution of small molecules in

the cellular biomass [3]. Metabolomics could provide the needed links between the complex metabolite mixtures in traditional herbal medicines and molecular pharmacology [4] and has great potential in the development of active secondary metabolites from medicinal plants as novel or improved phytotherapeutic agents [3].

*Echinacea* spp. (Asteraceae), endemic to North America, are widely used as herbal medicines and food supplements in Europe and North America. Previous studies have reported that *Echinacea* plants contain a variety of components including caffeic acid derivatives, alkamides, and polysaccharides [5], and the three *Echinacea* species, *E. purpurea*, *E. pallida*, and *E. angustifolia*, have some common or different phytochemical profiles in their roots, leaves or flowers [6–12]. Although a number of analytical methods for analyzing the chemical constituents of *Echinacea* plants have been reported, there is still frequent misidentification or substitution of the three species in the commercial *Echinacea* products [13,14]. This study provides an

<sup>☆</sup> This work was supported by institutional grant of Academia Sinica and national research program for genomic medicine (NSC 97-3112-B-001-020) of National Science Council of Taiwan, R.O.C.

\* Corresponding author. Agricultural Biotechnology Research Center, Academia Sinica, Taipei 115, Taiwan, ROC. Tel.: +886 2 26515028; fax: +886 2 26515028.

E-mail address: [lfshyur@ccvax.sinica.edu.tw](mailto:lfshyur@ccvax.sinica.edu.tw) (L.-F. Shyur).

efficient protocol to distinguish the three medicinal *Echinacea* species by a metabolomics approach, using supercritical fluid extraction (SFE) coupled with gas chromatography (GC)/mass spectrometry (MS) to generate the metabolite profiles of the three medicinal *Echinacea* species, grown under organic farming conditions, and then comparing them by various approaches, including principal component analysis (PCA) and generalized association plots (GAP).

*Echinacea* plant preparations are claimed to have several pharmacological effects, such as immune enhancement, anti-inflammation, and prevention of common cold [15]. Cyclooxygenase-2 (COX-2) catalyzes the synthesis of prostaglandins from the substrate arachidonic acid and has been also reported to be expressed within human tumor neovasculature as well as in neoplastic cells in human prostate, colon, breast, and lung cancer tissues [16,17]. Numerous reports have demonstrated that *Echinacea* constituents have inflammation-related bioactivities such as stimulation of cytokine production [18–21] or inhibition of COX-1 or COX-2 activity in vitro [22–25]. Recently, *Echinacea* alkalimides were reported to be a new class of cannabinomimetics modulating tumor necrosis factor  $\alpha$  (TNF- $\alpha$ ) gene expression via the cannabinoid type 2 (CB<sub>2</sub>) receptor [26,27]. Inducible nitric oxide synthase (iNOS) is one of the key enzymes producing nitric oxide (NO) and is expressed in response to a variety of pro-inflammatory cytokines and inflammatory agents such as lipopolysaccharide (LPS) at inflammatory sites [28]. Heme oxygenase-1 (HO-1), the rate-limiting enzyme in the breakdown of heme into carbon monoxide, iron and bilirubin, can be induced in various cell types such as endothelial cells, monocytes/macrophages, neutrophils, and fibroblasts by different stresses during the inflammatory response [29]. Specific metabolites displayed by the metabolomics study results in *Echinacea* plant extracts in this study were being further investigated for their inflammation-modulating activity on these important proinflammatory mediators, stress protein and/or cytokine/chemokine profiles in murine macrophages or skin system.

## 2. Materials and methods

### 2.1. Plant materials

*Echinacea purpurea*, *E. pallida*, and *E. angustifolia* were grown in Nantou Country, Taiwan, using organic farming conditions. Voucher specimens of the three *Echinacea* species, namely, Epu-1, Epa-1, and Ean-1, have been deposited at the Agricultural Biotechnology Research Center, Academia Sinica, Taipei, Taiwan. *Echinacea* plants at the flowering stage were harvested and separated into two groups (aerial parts and root parts) and then lyophilized.

### 2.2. Reagents and materials

3-(4,5-Dimethylthiazol-2-yl)-2,5-diphenyltetrazolium bromide (MTT), 12-O-tetradecanoylphorbol-13-acetate (TPA), LPS, 1,4-dithiothreitol (DTT), indomethacin, and aspirin were purchased from Sigma Chemical (St. Louis, MO, USA). Celecoxib (Celebrex) was from Pharmacia (Northumberland, UK). Silica gel (230–400 mesh), silica gel 60 F<sub>254</sub> thin-layer chromatography (TLC) and RP-18 F<sub>254s</sub> TLC plates were from Merck (Darmstadt, Germany), and RP-18 silica gel (75C<sub>18</sub>-OPN) was from Cosmosil (Kyoto, Japan). All other chemicals and solvents were reagent or high-performance liquid chromatography (HPLC) grade. Antibody sources are given below in the appropriate section.

### 2.3. Supercritical fluid extraction

Supercritical fluid extraction of *Echinacea* root or aerial tissues were performed using an ISCO SFE System 1220 (Lincoln, NE), with supercritical CO<sub>2</sub> as extraction fluid. One-gram samples of lyophilized tissue were extracted at 60°C for 30 min under a pressure of 3500 psi with an average CO<sub>2</sub> flow of 1.5 ml/min. The extracts were collected and air-dried over nitrogen gas, and dissolved in ethyl acetate for further analysis.

### 2.4. GC/MS analysis

GC/MS analyses were performed using a ThermoFinniganTrace GC 2000 equipped with a Polaris Q mass detector and the Xcalibur software system. A Supelcowax-10 fused silica capillary column (30 m×0.25 mm, film thickness 0.25  $\mu$ m) was used. The oven temperature was initiated at 50°C for 5 min then increased at a rate of 5°C/min to

280°C and held for 5 min. The injector and ion source temperatures were 230°C and 200°C, respectively. Helium was used as the carrier gas at 1 ml/min. The mass spectrometer was operated in electron impact mode (70 eV). Data acquisition was performed in the full scan mode from *m/z* 50–650 with a scan time of 0.58 s.

### 2.5. Clustering and visualization

Two multivariate statistical analysis and visualization methods, namely, biplot [30,31] and generalized association plots GAP [32,33], were used to analyze the GC/MS data of 15 extracts from *E. purpurea*, *E. pallida*, and *E. angustifolia* roots (5 independent root extracts from each species). A base 10 logarithm transformation was applied to peak area data for scaling range of peak areas from 0–10<sup>8</sup> down to 0–8. Seventy-nine major compound peaks from each GC chromatogram (a 15-by-79 data matrix) were analyzed and displayed by GAP with two proximity matrices and two hierarchical clustering trees (dendrograms) for illustrating plant clusters and compound groups. Biplot is then used to display originally high-dimensional relative between-plant and between-compound structures with the interaction patterns of compound groups on plant clusters in a low (two) dimensional space.

### 2.6. High-performance liquid chromatography–electron spray ionization/mass spectrometry analysis of metabolite profiles of *E. purpurea* root extracts with various post-harvest or abiotic treatments

*E. purpurea* plants harvested at the same flowering stage were randomly divided into six experimental groups. Plant samples with leaves struck with a brush of metal needles one day before harvest were defined as the physical stress group. The drought stress group did not receive watering one week before harvest. For post-harvest treatment groups, the *Echinacea* plants were harvested and then shade-dried, sun-dried, or incubated at 42°C for 2 h before being lyophilized to dryness. Plant root or aerial tissue extracts were prepared by ultrasonic extraction. A ThermoFinnigan LCQ Advantage ion trap mass spectrometer (San Jose, CA, USA), coupled with an Agilent 1100 series liquid chromatograph system was employed for HPLC/electron spray ionization/mass spectrometry (ESI/MS) analysis at the Metabolomics Core Facility of the Agricultural Biotechnology Research Center, Academia Sinica, Taiwan. One-gram samples of lyophilized root tissue were ground and extracted with 10 ml MeOH for 15 min ultrasonically and then filtered through 0.22  $\mu$ m polytetrafluoroethylene (PTFE) membranes prior to injection into a RP-18 column [Phenomenex Luna 3  $\mu$ m C18(2), 150 mm×2.0 mm] at a flow rate of 0.2 ml/min. Eluting peaks were monitored by photodiode array (DAD) detector simultaneously at 210 and 254 nm for alkalimides and at 254 and 330 nm for phenolic constituents before MS injection. Chromatography of alkalimides used a gradient of MeOH in water: 40–40% from 0 to 5 min, 40–60% from 5 to 15 min and 60–100% from 15 to 60 min. The phenolic constituents were analyzed with gradient elution by 0.05% trifluoroacetic acid (TFA)/water (solvent A) and 0.05% TFA/MeOH (solvent B): 5–5% from 0 to 5 min, 5–20% from 5 to 30 min, 20–45% from 30–40 min and 45–50% from 40 to 50 min. Ionization was performed in the positive ion mode for all analyses.

### 2.7. Cell lines and culture conditions

Murine macrophage RAW 264.7 cell and human breast adenocarcinoma MCF-7 cell were obtained from the American Type Culture Collection (Rockville, MD, USA). RAW 264.7 cells were grown in Dulbecco's modified Eagle medium (DMEM) (Gibco/BRL, Grand Island, NY, USA), and MCF-7 cells were grown in RPMI 1640 medium (Gibco/BRL), both media supplemented with 10% heat-inactivated fetal bovine serum (Gibco/BRL), 100 U/ml penicillin and 100  $\mu$ g/ml streptomycin, in a 5% CO<sub>2</sub> incubator at 37°C in a humidified atmosphere.

### 2.8. Isolation of alkalimide (8/9) and cichoric acid from *E. purpurea*

Approximately 1.5 kg of fresh *E. purpurea* roots were extracted by 100% methanol (1.6 L×2) at room temperature. The total methanolic extract was evaporated in vacuum, suspended in 1.0 L of water and partitioned with ethyl acetate (1.0 L×3) to yield two fractions designated as ethyl acetate (EA) and water fractions. The water fraction was further partitioned with *n*-BuOH to obtain BuOH fraction. Each fraction was dried using rotary evaporator and lyophilized. The EA fraction was chromatographed on a silica gel column with a hexane–ethyl acetate gradient to yield Fractions 1–5. Of these, Fraction 3 contained an alkalimides mixture (Alk mix). Fraction 3 was subsequently separated on a RP-18 silica gel (75C<sub>18</sub>-OPN) column eluted with a H<sub>2</sub>O/MeOH gradient to give dodeca-2E,4E,8Z,10Z(E)-tetraenoic acid isobutylamides (8/9). The butanol fraction was chromatographed on Diaion gel with a H<sub>2</sub>O/MeOH solvent system, and further purified on a Sephadex LH-20 column eluted with 60% MeOH to give cichoric acid. The compound purity of alkalimides 8/9 and cichoric acid were of >95%. Chemical structures were identified by nuclear magnetic resonance (NMR) and mass spectral analyses and agreed with the data published previously [34].

### 2.9. Luciferase reporter assay

Chimeric luciferase reporter gene containing the full-length 5'-flanking promoter region (–1334–1 bp) of the human COX-2 promoter was employed for the study, following a method published elsewhere [35]. The promoterless pPGL-3-basic vector

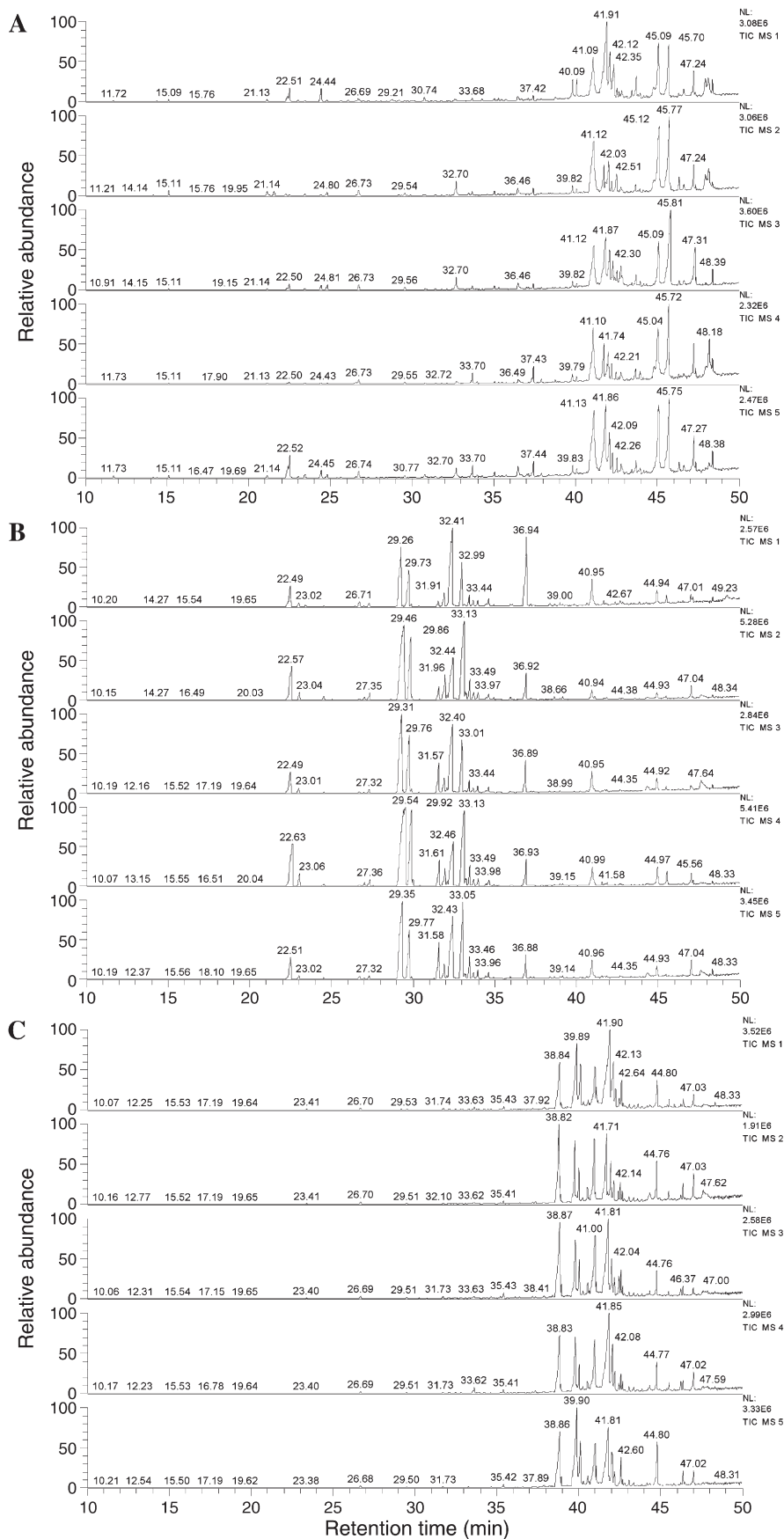


Fig. 1. Typical chromatography and metabolite profiling of root extracts of *E. purpurea* (A), *E. pallida* (B), and *E. angustifolia* (C) from supercritical fluid extraction. Five samples of each species were analyzed, with similar results.

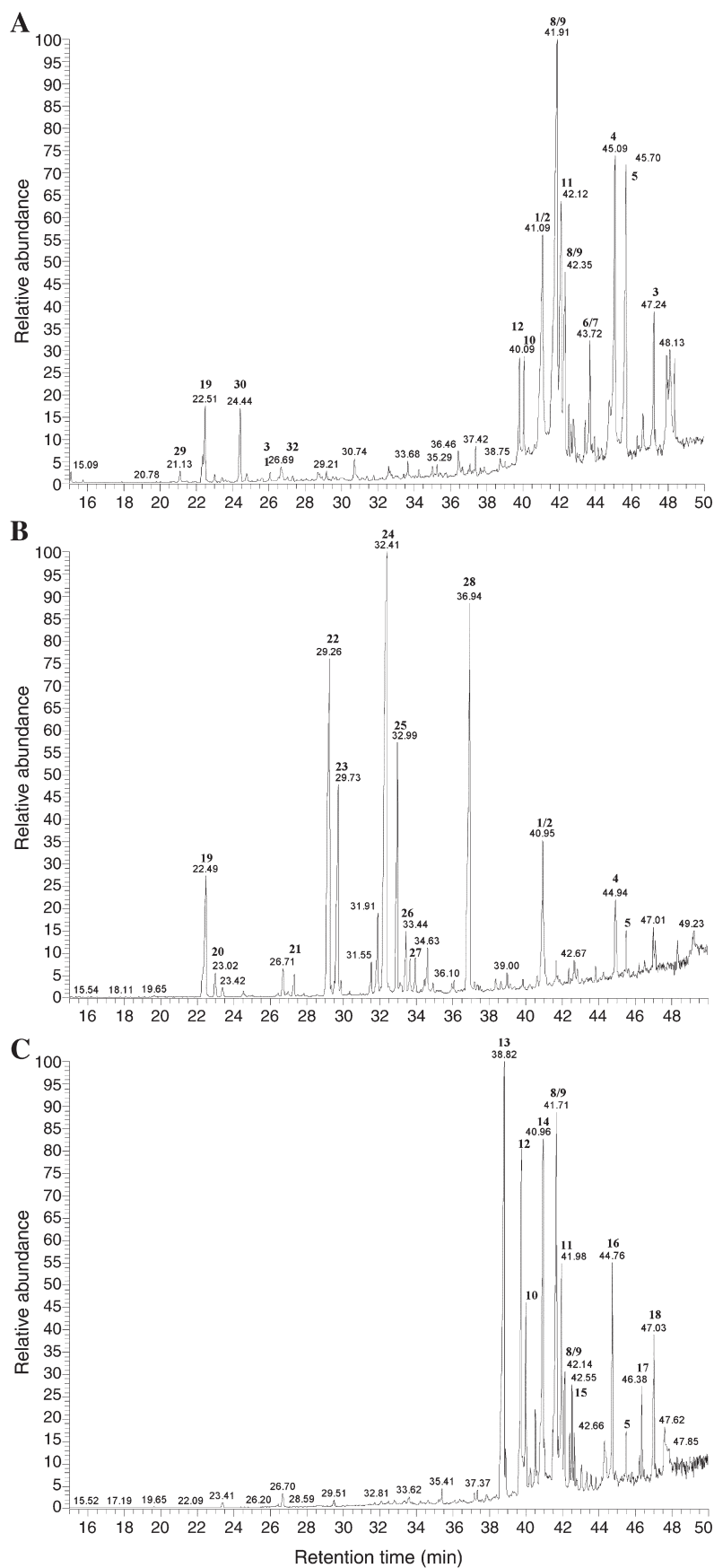


Fig. 2. GC/MS spectrometric analysis of the root extracts of *E. purpurea* (A), *E. pallida* (B), and *E. angustifolia* (C). Peaks were identified by comparison of their retention times and MS spectrum with the previous data in the literature.

was used as a negative control plasmid for luciferase assay. Briefly, MCF-7 cells were seeded in 24-well plates at a density of  $1.2 \times 10^5$  cells per well and cotransfected with pCOX-2-Luc and pPL-TK-Luc (Promega, Madison, WI, USA) plasmids using LipofectAMINE reagent (Invitrogen), as suggested by the manufacturer's protocol. The transfected cells were then treated with vehicle (0.001% dimethyl sulfoxide [DMSO]), 50 ng/ml TPA alone, or TPA mixed with test extracts or compounds at indicated concentrations for 6 h. Cell lysates were prepared using Passive Lysis Buffer (Promega) and then employed for luciferase activity assays. The promoter activity in arbitrary units was obtained from the ratio of firefly luciferase activity (pCOX-2-Luc) to that of *Renilla* luciferase (pPL-TK-Luc).

#### 2.10. Immunohistochemical study of COX-2 protein expression in mouse skin

Female ICR mice were supplied from the Laboratory Animal Center (College of Medicine, National Taiwan University, Taipei, Taiwan). Mice were supplied water feed ad libitum and kept on a 12-h light/dark cycle at  $22 \pm 2^\circ\text{C}$ . Mice were topically treated on their shaven backs with vehicle (acetone, 200  $\mu\text{l}$  per site) or TPA (10 nmol/200  $\mu\text{l}$  per site) for 4 h. For the extract or compound treatments, mice were pretreated with

extract or compound for 30 min first, further treated with TPA for 4 h and finally killed by cervical dislocation. The formalin-fixed, paraffin-embedded skin tissues were then stained according to the method of Chiang et al. [35].

#### 2.11. Measurement of NO production and cell viability

RAW 264.7 cells were seeded in 96-well plates at  $2 \times 10^5$  cells per well. The cells were treated with test compounds for 1 h and then incubated for 24 h in fresh DMEM with or without 1.0  $\mu\text{g}/\text{ml}$  LPS. Nitrite levels in RAW 264.7 cell culture medium were determined using the Griess reaction. Aliquots (100  $\mu\text{l}$ ) of cell culture supernatants were reacted with 100  $\mu\text{l}$  of Griess reagent (1:1 mixture of 0.1% *N*-(1-naphthyl) ethylenediamine in  $\text{H}_2\text{O}$  and 1% sulfanilamide in 5% phosphoric acid) in a 96-well plate, and absorbance at 540 nm was recorded using a plate reader (Labsystems Multiskan MS). Results were expressed as total  $\mu\text{M}$  nitrite produced in the three test groups: untreated cells, cells treated with LPS only, or cells treated with LPS plus phyto-extract or compound. RAW 264.7 cells ( $1 \times 10^4$ ) treated for 24 h with test extracts or compounds were examined for cell viability using the MTT based colorimetric assay [36]. Survival of macrophage cells after treatment was calculated by the following

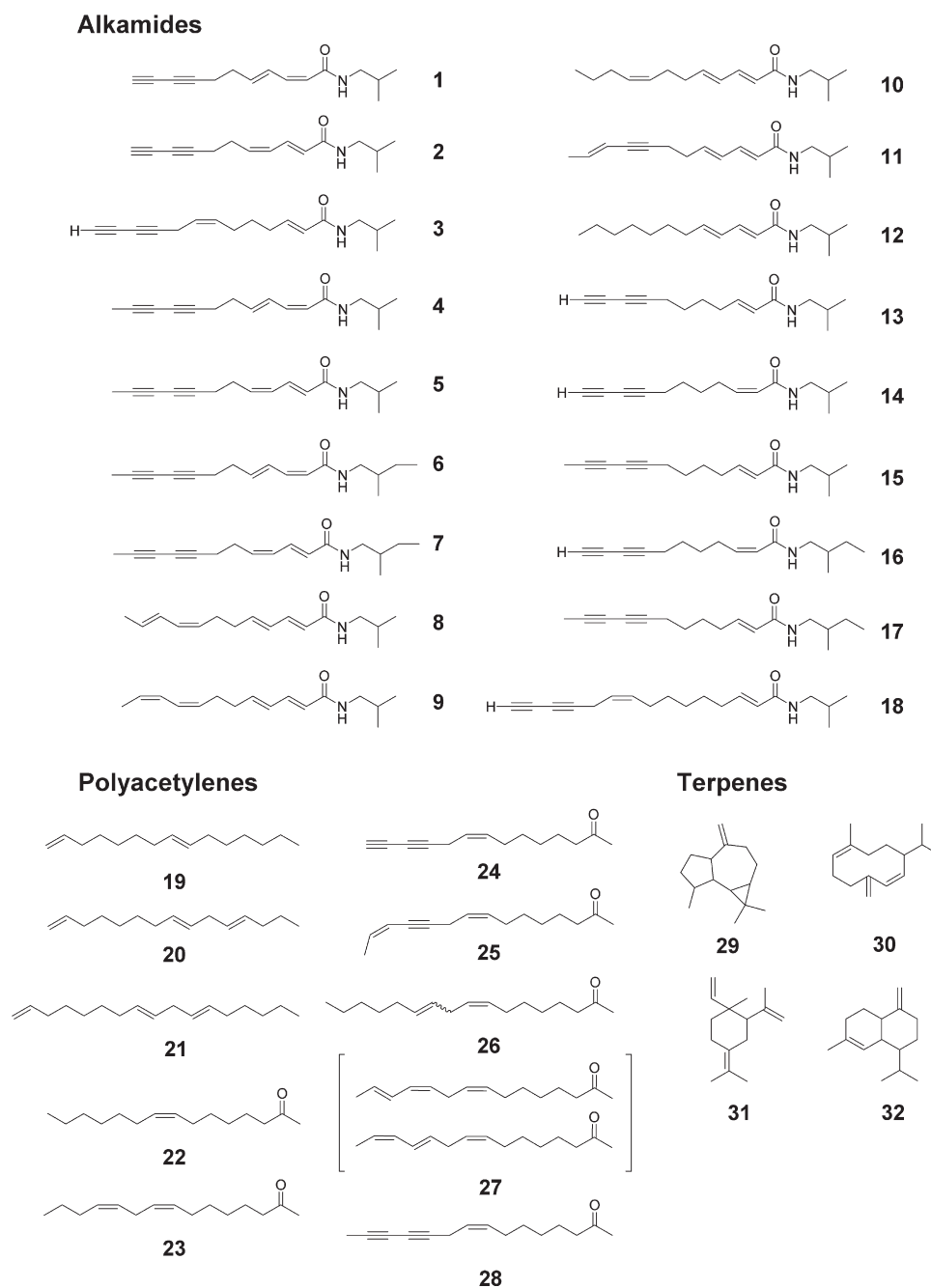


Fig. 3. Chemical structures of the 34 metabolites from three *Echinacea* species.



formula: viable cell number (%) =  $OD_{570}$  (treated cell culture) /  $OD_{570}$  (vehicle control)  $\times 100$ .

#### 2.12. COX activity assays

COX-2 and COX-1 enzymatic activity was measured using the chemiluminescent COX inhibitor screening assay kit (Cayman Chemical, Ann Arbor, MI, USA) according to the manufacturer's instructions.

#### 2.13. Quantification of cytokine profile with multicytokine detection system

Cytokine production profile in RAW 264.7 cells was analyzed using Beadlyte mouse 22-plex multicytokine detection system (Upstate) according to the manufacturer's instructions. Briefly, RAW 264.7 cells ( $2 \times 10^5$  cells per well) seeded in 96-well plates were treated with test compounds for 1 h and then incubated for 4 and 20 h, respectively, with or without cotreatment with 1.0  $\mu\text{g}/\text{ml}$  LPS; 50  $\mu\text{l}$  of cultured media were incubated with 25  $\mu\text{l}$  of bead solution overnight at 4°C and then incubated with biotin for 1.5 h. Finally, streptavidin-phycoerythrin was added and incubated in darkness for 30 min. Multi-wavelength fluorescence and cytokine concentrations were determined by laser detector (Luminex 100, Luminex, Austin, TX, USA) and Bio-Rad software (Bio-Rad, Hercules, CA, USA). Assays were performed in triplicate, and the obtained mean values were used for data analysis.

#### 2.14. Western blot analysis

Total cellular protein extracts were prepared according to Lo et al. [37]. The protein content was measured by the Bradford method (Bio-Rad Protein Assay Kit). Protein (20  $\mu\text{g}$ ) was separated by 5–20% gradient sodium dodecyl sulfate-polyacrylamide gel electrophoresis (SDS-PAGE) and then electrotransferred onto polyvinylidene difluoride membrane (Immobilon, Millipore, Bedford, MA, USA). The blots were incubated in blocking buffer (3% w/v skim milk in Tris-buffered saline) for 30 min and then incubated with monoclonal antibodies against G3PDH (Biogenesis, Poole, UK), COX-2 (Cayman Chemical), or iNOS (Santa Cruz Biotechnology, Santa Cruz, CA, USA) overnight at 4°C. After incubation with the appropriate antirabbit or antimouse IgG conjugated to horseradish peroxidase for 3 h at room temperature, the immunoreactive bands were visualized using enhanced chemiluminescence reagents (ECL, Amersham).

#### 2.15. Statistical analysis

Data are expressed as mean  $\pm$  S.D. Statistical significance of differences between treatments was determined by analysis of variance (ANOVA) with Fisher's post hoc test.  $P < .05$  was considered to be statistically significant.

### 3. Results

#### 3.1. GC/MS analysis and compound identification of plant extracts from three *Echinacea* species

Randomly selected root tissues harvested from flowering stage of the three medicinal species *E. purpurea*, *E. pallida*, and *E. angustifolia* (5 roots from each species) were collected and extracts prepared using SFE. The total yield of *E. purpurea*, *E. pallida*, and *E. angustifolia* extracts were 1.07%, 1.22% and 0.86%, respectively, by dry weight of root tissues. Equal amounts of extracts were dissolved in ethyl acetate and analyzed by GC/MS (Fig. 1). Very similar peak profiles were seen in root extracts from the same *Echinacea* species, while distinct chromatograms were observed between different species, suggesting an efficient and reproducible protocol of extraction and GC/MS analysis. The majority of the specific compounds in the spectra were verified on the basis of retention time and mass spectra and agreed with previously published spectral data [34,38–40] and the NIST and Wiley databases (Figs. 2 and 3). Alkamides were identified as the major lipophilic constituents in *E. purpurea* and *E. angustifolia* root extracts (Figs. 2A, C, and 3), particularly undeca- and dodecanoic acids with different degrees of unsaturation and bond configurations. Among them, isobutylamide was the major structural type, and some 2-methylbutylamides were also observed (Fig. 3). *E. pallida* extract contained far less alkamides than other two species, while a significant amount of ketoalkenes and ketoalkynes were detected (Figs. 2B and 3).

The metabolite distribution and relative content in the three *Echinacea* root extracts were calculated on the basis of the ratio of

individual compound peak area to the total peak areas in each chromatogram (Table 1). *E. purpurea* and *E. angustifolia* root extracts contained approximately 74.06% and 90.73% alkamides, respectively, while *E. pallida* root extract mainly composed of polyacetylenes (80.81%) and only 6.12% alkamides. Isomeric dodeca-2*E*,4*E*,8*Z*,10*Z*(*E*)-tetraenoic acid isobutylamides (**8/9**) were the major alkamides, comprising approximately 13.99% and 22.38%, respectively, of the *E. purpurea* and *E. angustifolia* root extracts, determined using a standard calibration curve of alkamide. 2-Monoene-8,10-diyenoic acid isobutylamide was only detected in *E. angustifolia* and some monoterpene constituents were mainly detected in *E. purpurea* (Fig. 3). These results demonstrate that SFE coupled with GC/MS analysis can be effectively applied for profiling and differentiating the chemical constituents existed in

Table 1  
A summary of metabolite distribution in the three medicinal *Echinacea* plants

Metabolites	<i>E. purpurea</i>	<i>E. pallida</i>	<i>E. angustifolia</i>
Alkamides	Relative content (%)		
undeca-2 <i>Z</i> ( <i>E</i> ),4 <i>E</i> ( <i>Z</i> )-dien-8,10-diyenoic acid isobutylamide ( <b>1/2</b> )	15.47	3.53	
trideca-2 <i>E</i> ,7 <i>Z</i> -dien-10,12-diyenoic acid isobutylamide ( <b>3</b> )	5.19		
dodeca-2 <i>Z</i> ,4 <i>E</i> -dien-8,10-diyenoic acid isobutylamide ( <b>4</b> )	12.89	1.92	
dodeca-2 <i>E</i> ,4 <i>Z</i> -dien-8,10-diyenoic acid isobutylamide ( <b>5</b> )	16.36	0.85	1.10
dodeca-2 <i>Z</i> ( <i>E</i> ),4 <i>E</i> ( <i>Z</i> )-en-8,10-diyenoic acid 2-methylbutylamide ( <b>6/7</b> )	1.92		
dodeca-2 <i>E</i> ,4 <i>E</i> ,8 <i>Z</i> ,10 <i>E</i> ( <i>Z</i> )-tetraenoic acid isobutylamide ( <b>8/9</b> )	11.74		20.64
dodeca-2 <i>E</i> ,4 <i>E</i> ,8 <i>Z</i> ,10 <i>Z</i> ( <i>E</i> )-tetraenoic acid isobutylamide ( <b>9/8</b> )	2.25		1.74
dodeca-2 <i>E</i> ,4 <i>E</i> ,8 <i>Z</i> -trienoic acid isobutylamide ( <b>10</b> )	0.74		5.02
dodeca-2 <i>E</i> ,4 <i>E</i> ,10 <i>E</i> -trien-8-ynoic acid isobutylamide ( <b>11</b> )	6.07		5.29
dodeca-2 <i>E</i> ,4 <i>E</i> -dienoic acid isobutylamide ( <b>12</b> )	1.43		14.85
undeca-2 <i>Z</i> ( <i>E</i> )-en-8,10-diyenoic acid isobutylamide ( <b>13</b> )			16.66
undeca-2 <i>E</i> ( <i>Z</i> )-en-8,10-diyenoic acid isobutylamide ( <b>14</b> )			12.05
dodeca-2 <i>E</i> -en-8,10-diyenoic acid isobutylamide ( <b>15</b> )			4.35
undeca-2 <i>Z</i> -en-8,10-diyenoic acid 2-methylbutylamide ( <b>16</b> )			4.94
dodeca-2 <i>E</i> -en-8,10-diyenoic acid 2-methylbutylamide ( <b>17</b> )			1.64
pentadeca-2 <i>E</i> ,9 <i>Z</i> -dien-12,14-diyenoic acid isobutylamide ( <b>18</b> )			2.45
Polyacetylenes			
pentadeca-1,8-diene ( <b>19</b> )	1.85	6.15	
pentadeca-1,8,11-trien ( <b>20</b> )		0.95	
heptadeca-1,8,11-triene ( <b>21</b> )		0.60	
pentadeca-8 <i>Z</i> -en-2-one ( <b>22</b> )		24.02	
pentadeca-8 <i>Z</i> ,11 <i>Z</i> -dien-2-ol ( <b>23</b> )		11.52	
tetradeca-8 <i>Z</i> -en-11,13-diyn-2-one ( <b>24</b> )		16.44	
pentadeca-8 <i>Z</i> ,13 <i>Z</i> -dien-11-yn-2-ol ( <b>25</b> )		12.96	
heptadeca-8 <i>Z</i> ,11-dien-2-one ( <b>26</b> )		1.76	
pentadeca-8 <i>Z</i> ,11,13-trien-2-ol ( <b>27</b> )		0.79	
pentadeca-8 <i>Z</i> -en-11,13-diyn-2-one ( <b>28</b> )		5.62	
Terpenes			
aromadendren ( <b>29</b> )	0.44		
germacrene-D ( <b>30</b> )	0.87		
$\gamma$ -gurjunene ( <b>31</b> )	0.27		
p-menth-1-ene-6-ol ( <b>32</b> )	0.32		

Peak numbering corresponds to Fig. 2.<sup>a</sup>

<sup>a</sup> The relative content of each peaks were calculated on the basis of the ratio of individual compound peak area to the total peak areas in each chromatogram.

root extracts of these three *Echinacea* species. The aerial parts of the three *Echinacea* species were also analyzed using the same protocols; however, very few detectable peaks were seen, suggesting that the aerial portion of *Echinacea* plants contain very little alkalimides (data not shown).

### 3.2. Metabolite clustering and visualization of the three medicinal *Echinacea* species using biplot and generalized association plots GAP

GAP and biplot analyses were used to analyze the metabolites distribution and content in *E. purpurea*, *E. pallida*, and *E. angustifolia*

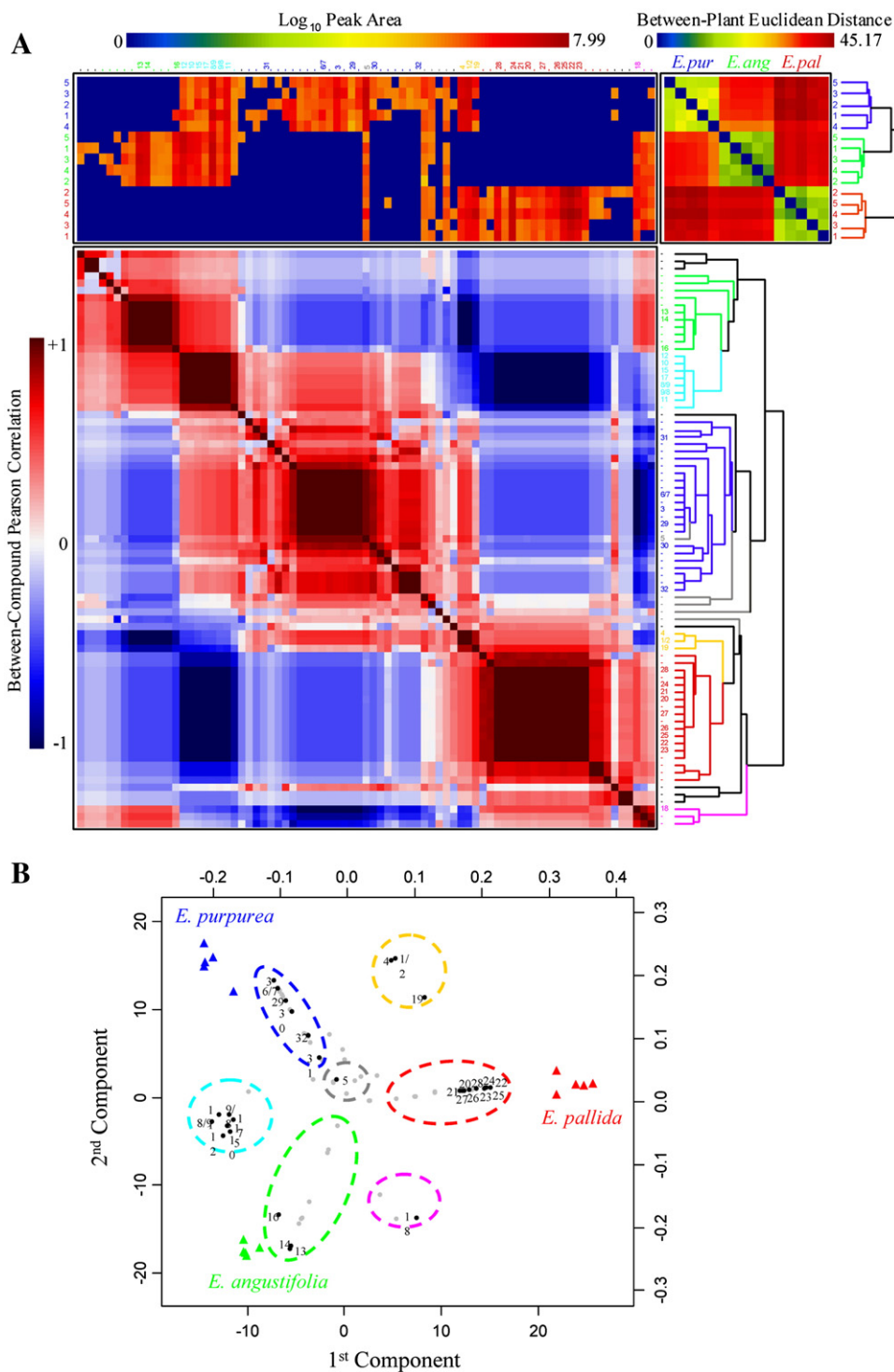


Fig. 4. Metabolite clustering and visualization of 15 plants from three *Echinacea* species [*E. purpurea* (blue triangles), *E. pallida* (red triangles), and *E. angustifolia* (green triangles)] with 79 phytocompounds: observed in *E. purpurea* only (blue lines or dashed circles), *E. pallida* only (red lines or dashed circles), and *E. angustifolia* only (green lines or dashed circles); *E. purpurea/angustifolia* shared compounds (cyan lines or dashed circles), *E. purpurea/pallida* shared compounds (orange lines or dashed circles), and *E. angustifolia/pallida* shared compounds (magenta lines or dashed circles); *E. purpurea/angustifolia/pallida* shared compounds (grey lines or dashed circles) using two statistical and visualization methods. (A) Generalized Association Plots (GAP). (B) Biplot display.

root tissues with base 10 logarithm transformed peak area of seventy-nine compounds. We have developed a GAP method to analyze plant metabolites. GAP is capable of providing five levels of information: (1) a raw score for every single plant/compound combination (15-by-79 matrix); (2) individual plant score-vectors across all compounds (15 rows) and individual compound-vectors of all plants (79 columns); (3) an association score for every plant-plant (15-by-15 matrix) and compound-compound relationship (79-by-79 matrix); (4) a grouping structure for compounds (dendrogram for compounds) and clustering effect for plants (dendrogram for plants); and (5) an interaction

pattern of plant-clusters on compound-groups. Seventy-nine highly reproducible compound peaks detected by GC/MS in each chromatogram from individual root extract (5 root extracts from each species for 15 root extracts in total) were analyzed and expressed as  $\log_{10}$  (peak intensity). The GAP display in Fig. 4A has three matrix maps permuted by two dendrograms. Two hierarchical clustering trees (HCTs) with dendrograms are built on the between-plant Euclidean distance matrix (15-by-15) and between-compound Pearson correlation matrix (79-by-79), respectively for permuting these two corresponding proximity matrices and the raw data ( $\log_{10}$  peak-

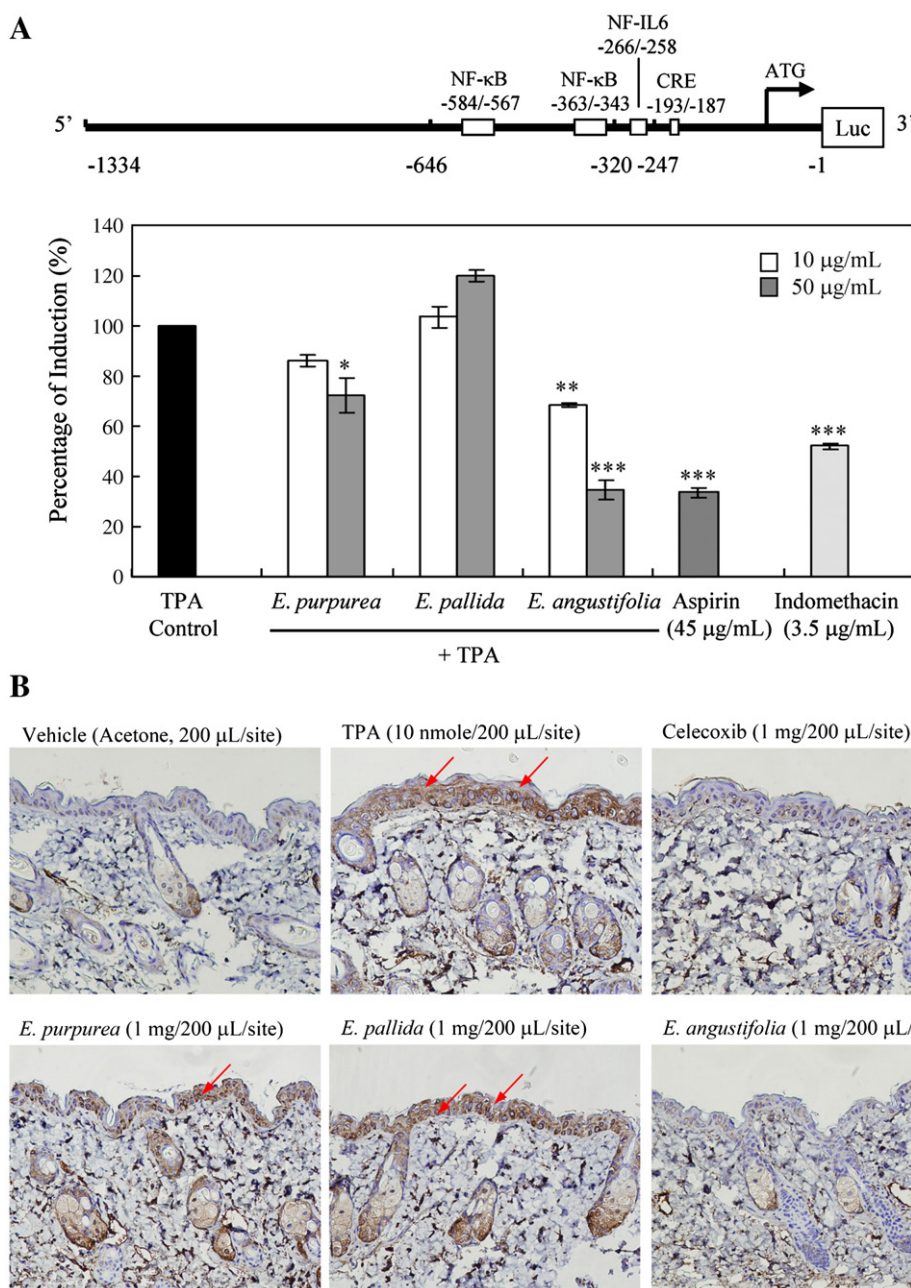


Fig. 5. Characterization of the effect of three *Echinacea* species on transcriptional activities of the *cox-2* promoter. (A) Human breast adenocarcinoma MCF-7 cells co-transfected with the full-length pCOX-2-Luc and internal control plasmid pRL-TK-Luc plasmid constructs were stimulated with TPA, in the absence or presence of the indicated concentrations of extracts. Control cells were not exposed to TPA. Aliquots (10  $\mu\text{g}$ ) of total protein lysate were subjected to dual luciferase reporter assay. The relative induction of *cox-2* promoter activity is shown, normalized to TPA treatment alone (100%). The significance of differences between means of different treatments were analyzed by Student's *t*-test. Significant inhibition is indicated by \*, \*\*, and \*\*\*, with a *P* value < .1, < .05, and < .01, respectively. Indo, indomethacin treatment. (B) Immunohistochemical study of the inhibitory effect of *Echinacea* roots extracts on TPA-induced COX-2 expression in mouse skin. Dorsal skin of female ICR mice was treated topically with acetone (vehicle control) or TPA (10 nmol in acetone) for 4 h or with the indicated concentrations of *Echinacea* extracts or celecoxib for 30 min before TPA treatment for 4 h. Immunohistograms were taken with an Olympus DP-70 camera on a Nikon ECLIPSE E800 microscope (magnification:  $\times 200$ ). The arrows indicate positive COX-2 staining (brown product).



area) matrix (15-by-79). In the construction of the two HCTs, average linkage distance option was used to compute the between-branch distances with flipping mechanic of intermediate nodes guided by rank-two elliptical seriation in Tien et al. [41].

The upper right distance matrix in rainbow scale clearly shows the distinct clusters of the three *Echinacea* species analyzed based on the Euclidean distance (although *E. purpurea* and *E. angustifolia* plants are closer to each other than to *E. pallida* plants) assisted by an HCT with color branches denoting three *Echinacea* species (blue for *E. purpurea*, green for *E. angustifolia* and red for *E. pallida*); the lower left correlation matrix in blue-red spectrum together with the colored branches also suggest roughly seven compound groups; the upper left plant-by-compound data matrix in rainbow spectrum then correlates the interaction pattern of the seven compound groups on the three plant clusters shown in Fig. 4B. Three compound groups were each expressed in only one *Echinacea* species (blue for *E. purpurea*, green

for *E. angustifolia* and red for *E. pallida*); the other three compound groups were shared by two *Echinacea* species (cyan for *E. purpurea/angustifolia*, orange for *E. purpurea/pallida*, and magenta for *E. angustifolia/pallida*), and one compound group was seen in all three *Echinacea* species (grey).

A biplot can simultaneously display originally high-dimensional relative between-plant and between-compound structures and their interaction patterns in a low dimensional space. The between-plant part is similar to a principal component analysis [42,43] for exploring the between-sample relationship while the between-compound part is related to a factor analysis [44] for understanding the between-compound structure. The biplot displayed in Fig. 4B contains two sets of symbols namely fifteen triangles one color groups for each plant with seventy-nine circles one for each compound. Color coding used for the biplot in Fig. 4B is identical to that used in Fig. 4A for GAP. Similar to the pattern in the GAP display for proximity matrix and data matrix in Fig. 4A, seven compound clusters can be easily identified in the biplot display of Fig. 4B. The red, green, and blue circled compound clusters contain those compounds only detected in *E. pallida*, *E. angustifolia*, and *E. purpurea* species, respectively. The cyan, magenta, and yellow clusters contain compounds shared by pairs of species. The middle grey cluster present compounds identified as common to all three *Echinacea* species.

Fig. 4A and B suggest that both GAP and biplot analyses can clearly differentiate the distribution of unique or common compounds in different medicinal plant species. While both GAP and biplot are capable in illustrating plant-clusters, compound-groups, and their interaction patterns, the exact compound-profile shared by each plant and the plant-profile affiliated to each compound are only available in the GAP display.

### 3.3. Comparative study of the extracts from three *Echinacea* species on COX-2 inhibition

COX-2 is an important inducible enzyme responsible for the production of a large amount of proinflammatory prostaglandins at an inflammatory site. We were interested in any correlation between the metabolite profile and major metabolites of specific root extracts with their potential anti-inflammatory bioactivity. Luciferase reporter gene activity driven by the 12-*O*-tetradecanoylphorbol-13-acetate (TPA)-induced COX-2 promoter in MCF-7 cells was employed as a primary system to compare the bioactivity of the root extracts from the three *Echinacea* species. Fig. 5A shows that *E. angustifolia* extract at 10 and 50  $\mu\text{g/ml}$  suppressed TPA-induced full-length COX-2 promoter activity (100%) in MCF-7 cells to 67% ( $P < .05$ ) and 34% ( $P < 1$ ) of control, respectively. Aspirin (45  $\mu\text{g/ml}$ ) and indomethacin

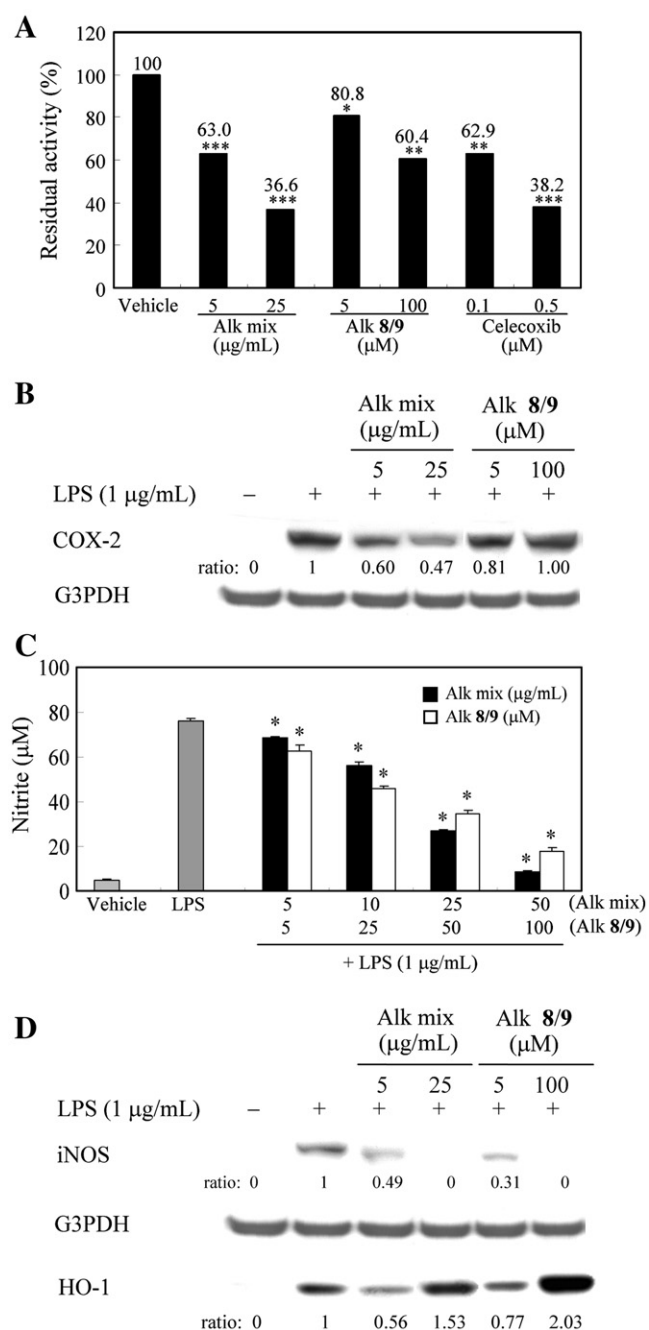


Fig. 6. Effect of alkamides on COX-2 enzymatic activity and expression, nitric oxide (NO) production and iNOS protein expression in RAW 264.7 cells. (A) Test compounds at the indicated concentrations were incubated with COX-2 enzyme and substrates, and COX-2 activity measured. Celecoxib was used as a positive control. The data are representative of three experiments and expressed as mean  $\pm$  S.D. Significant inhibition is indicated by \*, \*\*, and \*\*\*, with a  $P$  value  $< .05$ ,  $< .01$ , and  $< .005$ , respectively. (B) Cells were treated with the indicated concentrations of test compounds for 1 h, then LPS (1  $\mu\text{g/ml}$ ) was added for 18 h. Total cellular protein (20  $\mu\text{g}$ ) was resolved by SDS-PAGE then transferred to PVDF membrane and detected with antibody against COX-2 protein. COX-2 protein levels were normalized to G3PDH. (C) Effect of alkamide mixtures and 8/9 on LPS-induced NO production. Cells were treated with or without the indicated concentrations of test compound in 0.5% DMSO for 1 h, then LPS (1  $\mu\text{g/ml}$ ) was added and incubated for a further 24 h. Vehicle control was treatment with 0.5% DMSO only. NO in the culture medium was measured as described in Materials and methods. Cells were treated with or without the indicated concentration of test compounds for 24 h and percentage of cell viability was calculated. The data are expressed as mean  $\pm$  SD ( $n=3$ ). Student's  $t$ -test was used to analyze significance of differences, where \* indicates  $P$ -value  $< .001$ . (D) Effect of test compounds on LPS-induced iNOS and HO-1 protein expression in RAW264.7 cells. Total cellular protein (20  $\mu\text{g}$ ) was resolved by SDS-PAGE then transferred to PVDF membrane and detected with specific antibodies. iNOS and HO-1 protein expression were normalized to G3PDH levels (internal control).

(3.5 µg/ml), used as reference controls in this experiment, suppressed COX-2 promoter activity to 30–50% of the TPA control ( $P < 1$ ). Approximately 72% promoter activity was detected when transfected MCF-7 cells were treated with 50 µg/ml *E. purpurea* root extract ( $P < 1$ ), while the *E. pallida* root extract did not show any suppressive effect on COX-2 promoter activity at the same test concentration. The major differences in suppression of the TPA-induced *cox-2* promoter activity between the root extracts of *E. purpurea* and *E. angustifolia* are likely to be because the total content of alkamides is greater in root tissues of *E. angustifolia* than in *E. purpurea* (90.73% vs. 74.06%, Table 1). Additionally, Alk 8/9 and Alk 12 exist a larger amounts in *E. angustifolia* than *E. purpurea* (22.38% vs. 13.99% and 14.85% vs. 1.43%, respectively, shown in Table 1). When both compounds were tested at the same concentration 100 µM, Alk 12 was able to suppress a much more *cox-2* promoter activity induced by TPA than Alk 8/9 (60% vs. 24%, shown in Supplementary Fig. 1), indicating that at least Alk 12 makes a significant contribution to the detected difference in the *cox-2* promoter activity observed between the root extracts.

A TPA-induced mouse skin inflammation system and immunohistochemical analysis were employed to further evaluate the ability of the three *Echinacea* root extracts to inhibit COX-2 protein expression in vivo. After treatment with TPA (10 nmol/200 µl/site) for 4 h, COX-2 protein levels increased significantly in the epidermal layer of mouse skin compared to the vehicle control (Fig. 5B). At a dose of 1 mg/200 µl/site on mouse skin, the root extract of *E. angustifolia* significantly

attenuated TPA-induced COX-2 protein expression with effect comparable to that of celecoxib, a nonsteroidal anti-inflammatory agent and selective COX-2 inhibitor, at the same test concentration. Little or no inhibitory effect were observed for *E. purpurea* and *E. pallida* extracts, respectively (Fig. 5B). As shown in Table 1, alkamides were the major constituent components in the *E. purpurea* and *E. angustifolia* root supercritical fluid extracts, suggesting that alkamides could be the major active compounds for the anti-inflammatory activity in both *Echinacea* plants while polyacetylenes, the major constituent compounds in *E. pallida* roots, might not have any inhibitory effect on COX-2 expression at transcriptional and translational levels.

### 3.4. *Echinacea* alkamides inhibit COX-2 activity

In order to further characterize the anti-inflammatory activity of the specific alkamides, we prepared an alkamide-enriched fraction (designated Alk mix) and purified the major constituent 8/9 from the *E. purpurea* roots by liquid chromatography. Alk mix at 5 and 25 µg/ml inhibited 37% and 63% COX-2 enzymatic activity, Alk 8/9 (at 5 and 100 µM) inhibited COX-2 activity by 20–42%, while celecoxib at 0.1–0.5 µM inhibited activity by 40–62% (Fig. 6A). No detectable inhibition of COX-1 activity was observed with the Alk mix or Alk 8/9 (data not shown). Immunoblotting analysis of COX-2 protein expression in LPS-stimulated macrophages showed better suppression by Alk mix than Alk 8/9 (40–53% vs. 0–19%) at the same concentrations (Fig. 6B). These

Table 2  
Effect of alkamides and chichoric acid isolated from *E. purpurea* on cytokine expression profile in murine macrophage RAW 264.7

A. 4-h treatment							
Cytokine (pg/ml)	Cell (0.5% DMSO)	Alk mix		Alk 8/9		Cichoric acid	
		5 µg/ml	25 µg/ml	5 µM	100 µM	50 µM	100 µM
<b>Pro-inflammatory</b>							
TNF-α	459	331 (1.4) <sup>a</sup>	252 (1.8) <sup>b</sup>	403 (1.1)	214 (2.1)	329 (1.4)	347 (1.3)
IL-6	3.15	2.1 (1.5)	2.21 (1.4)	2.62 (1.2)	1.55 (2.0)	1.75 (1.8)	2.64 (1.2)
<b>Immunoregulatory</b>							
IL-10	12.8	9.91 (1.3)	11.9 (1.1)	7.52 (1.7)	1.09 (1.2)	7.02 (1.8)	12.7 (1.0)
IL-12p70	16.9	6.53 (2.6)	<2.3 <sup>c</sup> (>7.3)	<2.3 (>7.3)	<2.3 (>7.3)	<2.3 (>7.3)	13.7 (1.2)
IL-13	6.54	3.37 (1.9)	2.76 (2.4)	2.76 (2.4)	4.41 (1.5)	1.97 (3.3)	5.14 (1.3)
VEGF	2.96	1.48 (2.0)	1.21 (2.4)	2.35 (1.3)	0.6 (4.9)	1.71 (1.7)	1.71 (1.7)
<b>Chemokine</b>							
MCP-1	4450	2390 (1.9)	2290 (1.9)	3700 (1.2)	1620 (2.7)	3510 (1.3)	6450 (1.4)
MIP-1β	235	181 (1.3)	102 (2.3)	219 (1.1)	82.1 (2.9)	228 (1.0)	210 (1.1)
RANTES	4850	2110 (2.3)	1940 (2.5)	4350 (1.1)	1650 (2.9)	4790 (1.0)	5200 (1.1)
B. 20-h treatment							
Cytokine (pg/ml)	Cell (0.5% DMSO)	Alk mix		Alk 8/9		Cichoric acid	
		5 µg/ml	25 µg/ml	5 µM	100 µM	50 µM	100 µM
<b>Pro-inflammatory</b>							
TNF-α	896	387 (2.3) <sup>a,b</sup>	332 (2.7)	533 (1.7)	366 (2.4)	920 (1.0)	430 (2.1)
IL-1α	51	25.5 (2.0)	31.3 (1.6)	38 (1.3)	27.4 (1.9)	65.5 (1.3)	42.1 (1.2)
IL-6	4.11	1.21 (3.4)	1.38 (3.0)	2.19 (1.9)	1.96 (2.1)	4.33 (1.1)	2.6 (1.6)
<b>Immunoregulatory</b>							
IL-10	21.1	4.6 (4.6)	6.51 (3.2)	13.5 (1.6)	8.78 (2.4)	13.6 (1.6)	13.5 (1.6)
IL-12p70	25.4	<2.3 <sup>c</sup> (>11)	<2.3 (>11)	<2.3 (>11)	<2.3 (>11)	36.5 (1.4)	15.6 (1.6)
IL-13	13.7	3.99 (3.4)	4.2 (3.3)	5.46 (2.5)	2.56 (5.4)	5.78 (2.4)	7.62 (1.8)
VEGF	10.1	5.26 (1.9)	2.99 (3.4)		0.9 (11.2)	5.52 (1.8)	
<b>Chemokine</b>							
MCP-1	4890	1710 (2.9)	2120 (2.3)	3180 (1.5)	2360 (2.1)	9060 (1.9)	6480 (1.3)
MIP-1β	1300	381 (3.4)	132 (9.8)	656 (2.0)	163 (8.0)	1020 (1.3)	624 (2.1)
RANTES	8350	3020 (2.8)	1800 (4.6)	7000 (1.2)	2690 (3.1)	6200 (1.3)	7750 (1.1)

<sup>a</sup> Data in parentheses are relative change of compound treatment compared to vehicle (0.5% DMSO) control; up-regulations are shown as italics.

<sup>b</sup> Relative changes of 1.5 times or more are shown by shaded blocks.

<sup>c</sup> The lowest detectable level of IL-12p70 is 2.3 pg/ml in the assay system.

results suggest that other alkamide(s) present in Alk mix, apart from **8/9**, also contributed to the inhibition of COX-2 activity and protein expression.

### 3.5. Echinacea alkamides significantly inhibit NO production and iNOS protein expression in LPS-stimulated macrophage

The anti-inflammatory effect of alkamides on LPS-induced nitric oxide (NO) production and iNOS expression in RAW 264.7 cells was studied. Alk mix and Alk **8/9** induced a dose-dependent inhibition ( $P < 0.001$ ) of nitrite production with  $IC_{50}$  of 18.11  $\mu\text{g/ml}$  and 36.43  $\mu\text{M}$ , respectively (Fig. 6C). Western blot analysis also demonstrated significant inhibition of LPS-induced iNOS protein expression by

alkamides. Following incubation with either 5  $\mu\text{g/ml}$  Alk mix or 5  $\mu\text{M}$  Alk **8/9**, the level of iNOS protein was reduced by approximately 50% and 70%, and complete inhibition was observed with 25  $\mu\text{g/ml}$  Alk mix and 100  $\mu\text{M}$  Alk **8/9** (Fig. 6D). Thus, the inhibition of NO production by alkamides in LPS-stimulated macrophages is partly mediated by suppressing the expression of iNOS. The levels of HO-1 were increased by the higher concentrations of both alkamide treatments.

### 3.6. Effects of alkamides on cytokine/chemokine profiles in murine macrophage with or without LPS stimulation

The effects of alkamides on cytokines or chemokines secretion in RAW 264.7 cells with or without LPS stimulation were evaluated

Table 3

Effect of alkamides and cichoric acid isolated from *E. purpurea* on cytokine expression profile in LPS-stimulated macrophage RAW 264.7 cells

A. 4-h treatment								
Cytokine (pg/ml)	Control	LPS (1 $\mu\text{g/ml}$ )	+LPS (1 $\mu\text{g/ml}$ )					
			Alk mix		Alk <b>8/9</b>		Cichoric acid	
			5 $\mu\text{g/ml}$	25 $\mu\text{g/ml}$	5 $\mu\text{M}$	100 $\mu\text{M}$	50 $\mu\text{M}$	100 $\mu\text{M}$
<b>Pro-inflammatory</b>								
TNF- $\alpha$	459	753	918 (1.2) <sup>a</sup>	311 (2.4) <sup>b</sup>	765 (1.0)	463 (1.6)	617 (1.2)	621 (1.2)
IL-1 $\alpha$	6.53	33.4	7.11 (4.7)	4.80 (7.0)	11.4 (2.9)	6.01 (5.6)	40.6 (1.2)	27.6 (1.2)
IL-1 $\beta$	29.8	61.6	70.1 (1.1)	63.0 (1.0)	47.8 (1.3)	46.1 (1.3)	80.5 (1.3)	61.1 (1.0)
IL-6	3.15	83.1	98.8 (1.2)	29.5 (2.8)	103 (1.2)	31.2 (2.7)	105 (1.3)	101 (1.2)
<b>Immunoregulatory</b>								
IL-2	7.55	15.9	13.9 (1.1)	7.41 (2.1)	11.7 (1.4)	7.27 (2.2)	17.5 (1.1)	17.4 (1.1)
IL-10	12.8	54.9	59.1 (1.1)	25.7 (2.1)	59.4 (1.1)	28.4 (1.9)	7.02 (7.8)	12.7 (4.3)
IL-12p70	16.9	25.4	36.5 (1.4)	<2.3 <sup>c</sup> (<11)	33.6 (1.3)	13.1 (1.9)	19.3 (1.3)	22.4 (1.1)
<b>Chemokine</b>								
MCP-1	4450	6840	6300 (1.1)	2430 (2.8)	6700 (1.0)	3350 (2.0)	25700 (3.8)	>43600 <sup>d</sup> (>6.4)
MIP-1 $\beta$	235	828	943 (1.1)	207 (4.0)	726 (1.1)	314 (2.6)	1050 (1.3)	909 (1.1)
RANTES	4850	>31600 <sup>e</sup>	>31600	3390 (>9.3)	>31600	>31600	>31600	>31600
B. 20-h treatment								
Cytokine (pg/ml)	Control	(1 $\mu\text{g/ml}$ ) LPS	+ LPS (1 $\mu\text{g/ml}$ )					
			Alk mix		Alk <b>8/9</b>		Cichoric acid	
			5 $\mu\text{g/ml}$	25 $\mu\text{g/ml}$	5 $\mu\text{M}$	100 $\mu\text{M}$	5 $\mu\text{M}$	100 $\mu\text{M}$
<b>Pro-inflammatory</b>								
TNF- $\alpha$	896	2450	1540 (1.6) <sup>a,b</sup>	685 (3.6)	1400 (1.8)	682 (3.6)	1310 (1.9)	1250 (2.0)
IL-1 $\alpha$	6.92	59.1	45.0 (1.3)	42.6 (1.4)	44.5 (1.3)	18.5 (3.2)	45.5 (1.3)	42.6 (1.4)
IL-1 $\beta$	51.0	128	122 (1.0)	127 (1.0)	113 (1.1)	77.8 (1.6)	126 (1.0)	105 (1.2)
IL-6	4.11	>50003	2430 (2.1)	1090 (4.6)	4410 (1.1)	839 (6.0)	>5000 (1.0)	4040 (1.2)
<b>Immunoregulatory</b>								
IL-2	7.75	22.8	21.2 (1.1)	8.75 (2.6)	20.0 (1.1)	7.73 (2.9)	34.4 (1.5)	29.8 (1.3)
IL-10	21.1	960	1120 (1.2)	111 (8.6)	1310 (1.4)	43.7 (22)	1050 (1.1)	1130 (1.2)
IL-12p70	25.4	103	54.5 (1.9)	28.9 (3.6)	66.0 (1.6)	34.8 (3.0)	72.5 (1.4)	66.0 (1.6)
IL-13	13.7	24.1	22.9 (1.1)	23.4 (1.0)	24.6 (1.0)	11.2 (2.2)	20.7 (1.2)	24.8 (1.0)
VEGF	10.1	24.9	15.7 (1.6)	5.75 (4.3)	26.9 (1.1)	7.70 (3.2)	6.59 (3.8)	16.2 (1.5)
GM-CSF	6.73	597	174 (3.4)	8.62 (6.9)	382 (1.6)	90.0 (6.6)	565 (1.1)	621 (1.0)
<b>Chemokine</b>								
MCP-1	4890	>43600 <sup>c</sup>	13100 (>3.3)	4180 (>10.4)	>43600 (1.0)	14000 (>3.1)	>43600 (1.0)	>43600 (1.0)
MIP-1 $\beta$	1300	34800	15600 (2.2)	1790 (19.4)	11500 (3.0)	3360 (10.4)	>70600 (>2.1)	>70600 <sup>c</sup> (>2.1)
RANTES	8350	>31600 <sup>c</sup>	25800 (1.2)	1660 (19.0)	>31600 (1.0)	7030 (4.5)	>31600 (1.0)	>31600 (1.0)
KC	6.83	15.4	12.6 (1.2)	12.6 (1.2)	12.1 (1.3)	7.63 (2.0)	18.9 (1.2)	18.9 (1.2)

<sup>a</sup> Data in parentheses are relative change of compound + LPS treatment compared to LPS treatment only; up-regulations are shown as italics.

<sup>b</sup> Relative changes of 1.5 times or more are shown by shaded blocks.

<sup>c</sup> The highest detectable levels of IL-6, MCP-1, MIP-1, and RANTES are 5000, 43600, 70600, and 31600 pg/ml, respectively, in the assay system.

<sup>d</sup> The lowest detectable level of IL-12p70 in the assay system was 2.3 pg/ml.

<sup>e</sup> The highest detectable level of MCP-1 was 43600 pg/ml.

<sup>f</sup> The highest detectable level of RANTES was 31600 pg/ml.



using a Beadlyte mouse cytokine array assay. Cichoric acid was tested in parallel as a reference in this study. Twenty-two cytokines/chemokines [interleukin (IL)-1 $\alpha$ , IL-1 $\beta$ , IL-2, IL-3, IL-4, IL-5, IL-6, IL-7, IL-8, IL-10, IL-12p40, IL-12p70, IL-13, IL-15, TNF- $\alpha$ , GM-CSF, IFN $\gamma$ , eotaxin, MCP-1, RANTES, MIP-1 $\beta$ , and KC] on a single array were analyzed. Those molecules responsive to phytochemical treatment are summarized in Tables 2 and 3. An MTT viability assay confirmed that Alk mix, Alk 8/9, and cichoric acid did not have detectable cytotoxicity on macrophages at the tested concentrations (data not shown). The Alk mix (at 5 or 25  $\mu$ g/ml) and Alk 8/9 (at 100  $\mu$ M) suppressed the secretion of TNF- $\alpha$ , IL-1 $\beta$ , IL-6, IL-10, IL-12p70, IL-13, vascular endothelial growth factor (VEGF), MCP-1, MIP-1 $\beta$ , and RANTES in RAW 264.7 cells, with a more significant effect after a 20-h treatment than after a 4-h treatment (Table 2). Cichoric acid (100  $\mu$ M) down-regulated TNF- $\alpha$ , IL-6, IL-10, IL-12p70, IL-13, VEGF, and MIP-1 $\beta$  with 4- or 20-h treatments, with a near tenfold reduction in VEGF levels. These results suggest that alkamides and cichoric acid may modulate macrophage activity, mainly by suppression of cytokine and chemokine levels.

RAW 264.7 cells were stimulated with the bacterial endotoxin LPS for 4 h or 20 h. After 4 h, the levels in the culture medium of 7 cytokines and 3 chemokines (TNF- $\alpha$ , IL-1 $\alpha$ , IL-1 $\beta$ , IL-2, IL-6, IL-10, IL-12p70, MCP-1, MIP-1 $\beta$ , and RANTES) were significantly elevated (1.5- to 26-fold) (Table 3A), while after a longer time LPS stimulation (20 h), IL-13, VEGF, GM-CSF and KC were also increased (1.75- to 2.3-fold) (Table 3B) compared to cells treated with vehicle only. When LPS-challenged cells were treated with Alk mix (25  $\mu$ g/ml) or Alk 8/9 (100  $\mu$ M), the LPS-induced expression of all tested cytokines/chemokines was reduced, with a stronger effect from Alk 8/9 (Table 3B). Cichoric acid (100  $\mu$ M treatment for 4 h or 20 h), however, only inhibited LPS-induced IL-10 (4.3-fold), TNF- $\alpha$  (1.9-fold), and VEGF (3.8-fold) expression, with a mild elevation (1.5-fold) of LPS-induced IL-2 level and a 6.4-fold increase in MIP-1 $\beta$  level. These results indicate that compound alkamides are the key anti-inflammatory constituents in *Echinacea* plants.

### 3.7. HPLC-ESI/MS metabolite profiling of alkamides and phenolic compounds in *E. purpurea* roots under various post-harvest or abiotic treatments

We examined whether various treatments before or after plant harvesting can alter the specific alkamide or phenolic contents in *E. purpurea* roots. *E. purpurea* plants at the flowering stage were divided into 6 groups: untreated, physical stress (striking the leaves with a metal brush), simulated drought, 42°C treatment, shade-dried, and

sun-dried groups, and the metabolite profiles of the root extracts, prepared using ultrasonic extraction, were analyzed using HPLC-ESI/MS. Table 4 summarizes the changes in content of alkamides 1–12, cichoric acid and rutin (see also Fig. 7) quantified against a standard calibration curve of the respective compound and analyzed by one-way ANOVA. Total alkamides content in *E. purpurea* roots were decreased by all five treatments as compared to the untreated root extract; interestingly, the physical stress had the most dramatic effect, with a decrease in total alkamide content of up to 44%; decreases of 37.8, 34.7, 26.7, and 22.7% were observed in shade-dried, sun-dried, drought stress, and 42°C treatment, respectively (Table 4). Among the 12 alkamides, the changes of major alkamides 8/9 were statistically significant ( $P < 5$ ) in the physical stress, shade-dried and 42°C treatment groups (Fig. 7A).

The results of quantitative analysis of cichoric acid and rutin under various treatments show that shade-dried and sun-dried treatments drastically attenuated both compounds contents ( $P < 5$ ) in *E. purpurea* roots (73–92% decrease,  $P < 5$ ) (Table 4 and Fig. 7B). Surprisingly, the physical stress resulted in approximately 65% increase in rutin content ( $P < 5$ ). Together, these results suggest that environmental factors or post-harvest treatment can have some substantial effects on metabolites distribution in medicinal plants.

## 4. Discussion

*Echinacea* preparations were the top-selling herbal supplements or medicines in the past decade and represent the most common herbal immunomodulators (<http://nccam.nih.gov/>). Current commercial preparations sold under the name *Echinacea* may in fact be completely different preparations, using different extraction methods and plant parts or a mixture of plant varieties. It is clear, therefore, that there are still many challenges facing the rational use of *Echinacea*, such as determination of the most effective parts of the plant, and the differences in bioefficacy of the three most abundantly used species (<http://nccam.nih.gov/>). We therefore established here an efficient and highly reproducible extraction and analysis protocol for better quality control and species classification of *Echinacea* plant extracts using a metabolomics approach. The three *Echinacea* plants were grown under controlled and home-defined organic farming conditions and subjected to supercritical fluid extraction couple with GC/MS for enrichment of and analyzing lipophilic constituents in *Echinacea* roots. By employing PCA and biplot analyses, the distribution of unique and common compounds within the three medicinal plant species could be clearly differentiated (Fig. 4). Analysis of the bioefficacy of the metabolites identified by the

Table 4  
Effect of specific post-harvest or abiotic treatments on metabolites in *E. purpurea* root extracts<sup>a</sup>

Compound (mg/g)	Untreated	Physical	Drought	42°C treatment	Shade-dried	Sun-dried
<b>Alkamides</b>						
1	1.89±0.33	1.06±0.11	1.37±0.23	1.48±0.30	1.24±0.23	0.87±0.07
2	0.69±0.31	0.21±0.05	0.31±0.05	0.43±0.15	0.28±0.02	0.38±0.06
3	0.69±0.08	0.47±0.10	0.49±0.11	0.65±0.07	0.45±0.13	0.31±0.05
4	1.05±0.26	0.66±0.18	0.64±0.16	0.80±0.10	0.60±0.19	0.46±0.06
5	1.57±0.35	1.07±0.12	1.30±0.39	1.69±0.25	1.03±0.32	0.88±0.26
6	0.10±0.03	0.07±0.03	0.07±0.02	0.08±0.02	0.07±0.02	0.05±0.01
7	0.12±0.01	0.09±0.02	0.10±0.02	0.13±0.02	0.09±0.02	0.06±0.02
8/9	3.92±0.28	1.83±0.24	3.04±0.65	2.33±0.28	2.46±0.46	3.57±0.38
10	0.23±0.09	0.09±0.02	0.10±0.03	0.14±0.05	0.10±0.01	0.11±0.02
11	0.26±0.09	0.36±0.20	0.29±0.07	0.34±0.09	0.21±0.06	0.17±0.04
12	0.10±0.03	0.09±0.03	0.07±0.02	0.12±0.03	0.08±0.01	0.08±0.03
Total alkamides	10.62±1.20	5.99±0.54	7.78±0.62	8.21±1.00	6.61±0.75	6.94±0.33
Cichoric acid	29.30±7.82	32.30±11.92	26.39±3.64	23.09±10.12	7.81±3.53	2.35±1.41
Rutin	109.46±27.04	180.69±44.53	94.34±14.33	74.73±50.29	8.48±3.84	11.66±3.13
Total	138.75±26.18	212.99±50.05	120.73±14.38	97.82±59.29	16.29±5.21	14.01±2.72

<sup>a</sup> Values are means (S.D.). Mean levels of the compounds were measured as mg/g in dry weight ( $n=5$ ).

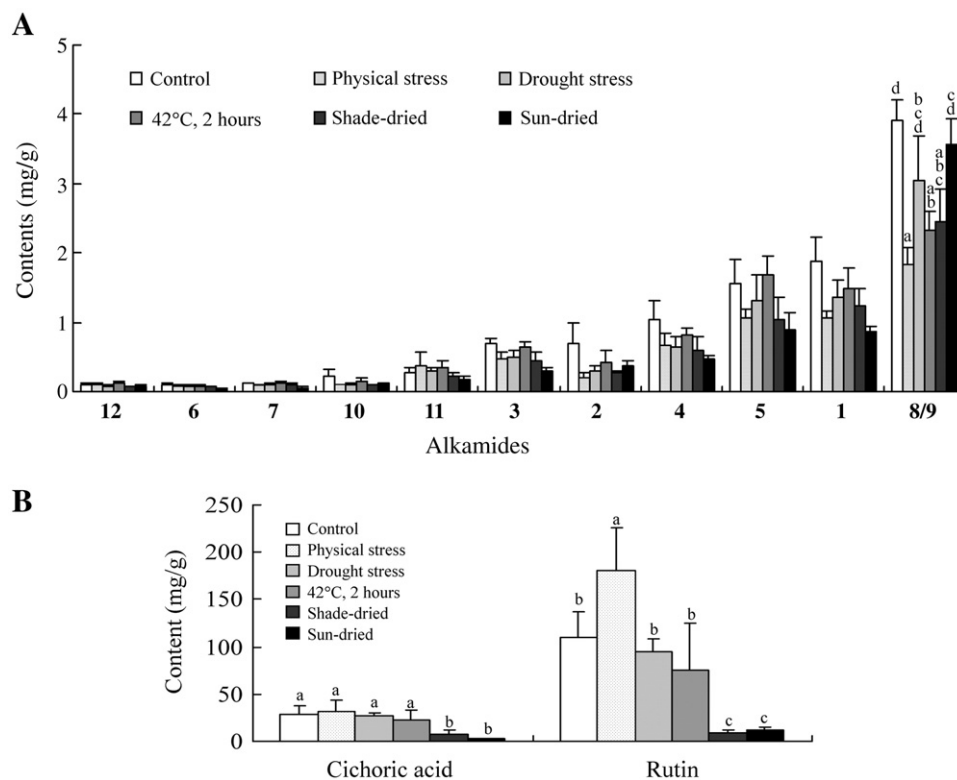


Fig. 7. Alkamide, cichoric acid and rutin levels in roots of *E. purpurea* with or without specific post-harvest abiotic treatments. Bars with a different letter are significantly different from each other ( $P < 5$ ) as determined by ANOVA. Values are means  $\pm$  SD from five extracts ( $n = 5$ ) in two independent determinations.

metabolomics profiling by cell- and gene-based assays demonstrated that the order of efficacy of the three plant root extracts was *E. angustifolia* > *E. purpurea* > *E. pallida* (Fig. 5). The abundant alkamides in both *E. angustifolia* and *E. purpurea* were then correlated with the observed anti-inflammatory activity in the extracts, in further bioactivity studies using an enriched alkamides mixture or major alkamides **8/9** (Fig. 6).

LPS from the outer membrane of Gram-negative bacteria can trigger potent inflammatory responses during endotoxemia, including induction of iNOS and COX-2 gene and/or protein expression and cytokines released [45,46]. Our results indicate that alkamides mixture (Alk mix) and its major constituents Alk **8/9** from *E. purpurea* can inhibit expression of both iNOS and COX-2 proteins, and NO production in LPS-stimulated murine macrophages. In comparison, the purified Alk **8/9** had less effect than the Alk mix, indicating that other alkamides present in Alk mix also contribute to these anti-inflammatory activities. Indeed, our preliminary data for a more recent study shows that Alk **12** has a higher effect than Alk **8/9** on suppression of transient COX-2 promoter activity induced by TPA in MCF-7 cells (60% vs. 24%, shown in Supplementary Fig. 1) and NO production ( $IC_{50} = 74.2$  vs.  $43.7 \mu\text{M}$ , data not shown) in LPS-stimulated macrophages. Previous studies have reported that *E. purpurea* aerial parts preparations induced IL-1, IL-10, and TNF- $\alpha$  secretion in human macrophages [21], and water extracts from *E. purpurea* stimulated non-adherent mouse splenocyte populations to produce TNF- $\alpha$ , IL-10 and MIP-1 $\alpha$  [19]. Likewise, *Echinacea* preparations, either enriched in polysaccharides or in alkamide and phenolic components, can reverse the expression changes of some inflammatory cytokines or chemokines in rhinovirus-infected epithelial cells, though treatment with either extract alone was also observed to induce some proinflammatory cytokines or chemokines expression in un-infected cells [18]. In this study, we observed that 4-h or 20-

h treatment of murine macrophages with an alkamide mixture from *E. purpurea* roots or with Alk **8/9** alone suppressed most proinflammatory cytokines or chemokines, while only moderate effect was seen with a 20-h cichoric acid treatment (Table 2). Similar alkamide suppression of LPS-induced cytokines/chemokines activity in macrophages was detected (Table 3), while cichoric acid only exhibited moderate suppression of TNF- $\alpha$  and VEGF secretion, and induction of MIP-1 $\beta$  (Table 3B). Alkamides **8/9** and **12** have been reported elsewhere to inhibit expression of TNF- $\alpha$  induced by LPS in human monocytes/macrophages via the CB<sub>2</sub> receptor [19,27], which supports part of our observed effects in murine macrophages. Together, these data clearly indicate that the alkamides are the anti-inflammatory constituents in *Echinacea* extracts, and suggest some potential for the therapeutic use of alkamides in endotoxemia or septic shock induced by LPS. Although cichoric acid has moderate inhibitory effects on proinflammatory cytokine/chemokine secretion, little effect was seen on COX-2 and iNOS expression (data not shown) in the same macrophages with LPS stimulation, implying cichoric acid may not play a role in LPS-related inflammatory disorders, but some other cell-mediated immunity.

Carbon monoxide, one the three byproducts of the catabolism of heme by HO, can inhibit the expression of LPS-induced proinflammatory cytokines both in vivo and in vitro [47,48]. The alkamide promotion of HO-1 expression in macrophages (Fig. 6D) may contribute to their inhibitory effect on the LPS-induced production of proinflammatory cytokines TNF- $\alpha$ , IL-1 $\alpha$ , and IL-6. Natural compound suppression of iNOS expression by enhancing HO-1 expression has been reported in previous studies [49–51]. Direct evidence to support and link such a cascade mode of action of alkamides on HO-1 and proinflammatory mediators awaits further studies.

Plant developmental stage, growing conditions, and post-harvest treatments may significantly influence the plant secondary



metabolite status in plants. These changes may also be directly correlated to the nutritional and functional values of vegetables or medicinal plants. We attempted in this study to investigate whether several simple treatments could affect the alkalamide and phenolics (i.e., cichoric acid and rutin) contents in *E. purpurea* roots (Table 4). In summary, the total alkalamide contents fell by 22% to 43% among the five different treatments. Although some reduction was seen in diynoic acid isobutylamide derivatives (1–4), the largest effects were on the most abundant compound, Alk 8/9, with statistically significant reductions following physical stress, heat treatment (42°C for 2 h) and shade-drying. Conversely, the physical stressing by striking the leaves with a brush of metal needles before harvest significantly increased the rutin content, by 65% (Table 4). Wounding by fresh-cutting has been reported elsewhere to increase the total phenolic content in lettuce leaf tissue [52,53] and in purple-flesh potatoes [54], and was correlated to an increase of phenylalanine ammonia lyase activity and antioxidant activity. Rutin is known to possess antioxidant activity, and a similar increase in antioxidant activity can be expected in the *E. purpurea* root tissue in the physical stress group. However, contradictory effects were observed for alkalamides and rutin in *E. purpurea*. It is possible that an appropriate abiotic stress or post-harvest treatment of the plant may be able to produce a product tailored to a specific pharmacological profile or other desired outcome. It will be interesting in future to investigate the signaling molecules, enzymes, and pathway(s) that regulate the biosynthesis of the alkalamides or the specific phenolic compound in terms that translate to their medical functions.

#### Acknowledgments

The authors are grateful to the High Field Nuclear Magnetic Resonance Center, National Science and Technology Program for Medical Genomics, Taiwan, for measurement of the NMR spectra. We thank Dr Harry Wilson, Academia Sinica, for his careful reading of the manuscript, and Miss Su-Shiang Lin for her technical assistant on *Echinacea* plants cultivation.

#### Appendix A. Supplementary data

Supplementary data associated with this article can be found, in the online version, at doi:10.1016/j.jnutbio.2009.08.010.

#### References

- Rochfort S. Metabolomics reviewed: a new “omics” platform technology for systems biology and implications for natural products research. *J Nat Prod* 2005;68:1813–20.
- Sumner LW, Mendes P, Dixon RA. Plant metabolomics: large-scale phytochemistry in the functional genomics era. *Phytochemistry* 2003;62:817–36.
- Shyur LF, Yang NS. Metabolomics for phytochemistry research and drug development. *Curr Opin Chem Biol* 2008;12:66–71.
- Wang M, Lamers RJ, Korthout HA, van Nesselrooij JH, Witkamp RF, van der Heijden R. Metabolomics in the context of systems biology: bridging traditional chinese medicine and molecular pharmacology. *Phytother Res* 2005;19:173–82.
- Bauer R. Chemistry, analysis and immunological investigations of *Echinacea* phytopharmaceuticals. In: Wagner H, editor. Immunomodulatory agents from plants. Boston (Mass): Birkhäuser Inc.; 1999. p. 41–88.
- Perry NB, van Klink JW, Burgess EJ, Parmenter GA. Alkamide levels in *Echinacea purpurea*: a rapid analytical method revealing differences among roots, rhizomes, stems, leaves and flowers. *Planta Med* 1997;63:58–62.
- He XG, Lin LZ, Bernart MW, Lian LZ. Analysis of alkalamides in roots and achenes of *Echinacea purpurea* by liquid chromatography-electrospray mass spectrometry. *J Chromatog A* 1998;815:205–11.
- Sioley BD, Urlichuk LJ, Tywin C, Coutts RT, Pang PKT, Shan JJ. Comparison of chemical components and antioxidant capacity of different *Echinacea* species. *J Pharm Pharmacol* 2001;53:849–57.
- Cech NB, Eleazer MS, Shoffner LT, Crosswhite MR, Davis AC, Mortenson AM. High performance liquid chromatography/electrospray ionization mass spectrometry for simultaneous analysis of alkalamides and caffeic acid derivatives from *Echinacea purpurea* extracts. *J Chromatog A* 2006;1103:219–28.
- Perry NB, Burgess EJ, Glennie VI. *Echinacea* standardization: analytical methods for phenolic compounds and typical levels in medicinal species. *J Agric Food Chem* 2001;49:1702–6.
- Gotti R, Pomponio R, Bertucci C, Cavrini V. Simultaneous analysis of the lipophilic and hydrophilic markers of *Echinacea* plant extracts by capillary electrophoresis. *J Sep Sci* 2002;25:1079–86.
- Bergeron C, Livesey JF, Awang DVC, Arnason JT, Rana J, Baum BR, et al. Quantitative HPLC method for the quality assurance of *Echinacea* products on the north American market. *Phytochem Anal* 2000;11:207–15.
- Gilroy CM, Steiner JF, Byers T, Shapiro H, Georgian W. *Echinacea* and truth in labeling. *Arch Intern Med* 2003;163:699–704.
- Raloff J. Herbal lottery: what's on a dietary supplement's label may not be what's in the bottle. *Sci News* 2003;163.
- Bauer R, Wagner H. *Echinacea* species as potential immunostimulatory drugs. In: Wagner H, Farnsworth NR, editors. Economic and Medicinal Plant Research, vol. 5. San Diego (Calif): Academic Press Inc.; 1991. p. 253–321.
- Masferrer JL, Leahy KM, Koki AT, Zweifel BS, Settle SL, Woerner BM, et al. Antiangiogenic and antitumor activities of cyclooxygenase-2 inhibitors. *Cancer Res* 2000;60:1306–11.
- Williams CS, Mann M, DuBois RN. The role of cyclooxygenases in inflammation, cancer, and development. *Oncogene* 1999;18:7908–16.
- Sharma M, Arnason JT, Burt A, Hudson JB. *Echinacea* extracts modulate the pattern of chemokine and cytokine secretion in rhinovirus-infected and uninfected epithelial cells. *Phytother Res* 2006;20:147–52.
- Hwang SA, Dasgupta A, Actor JK. Cytokine production by non-adherent mouse splenocyte cultures to *Echinacea* extracts. *Clin Chim Acta* 2004;343:161–6.
- Barrett B. Medicinal properties of *Echinacea*: a critical review. *Phytomedicine* 2003;10:66–86.
- Burger RA, Torres AR, Warren RP, Caldwell VD, Hughes BG. *Echinacea*-induced cytokine production by human macrophages. *Int J Immunopharmacol* 1997;19:371–9.
- Clifford LJ, Nair MG, Rana J, Dewitt DL. Bioactivity of Alkamides Isolated from *Echinacea purpurea* (L.) Moench. *Phytomedicine* 2002;9:249–53.
- Muller-Jakic B, Breu W, Probstle A, Redl K, Greger H, Bauer R. In vitro inhibition of cyclooxygenase and 5-lipoxygenase by alkalamides from *Echinacea* and *Achillea* species. *Planta Med* 1994;60:37–40.
- Raso GM, Pacilio M, Di Carlo G, Esposito E, Pinto L, Meli R. In-vivo and In-vitro anti-inflammatory effect of *Echinacea purpurea* and *Hypericum perforatum*. *J Pharm Pharmacol* 2002;54:1379–83.
- Hinz B, Woelkart K, Bauer R. Alkamide from *Echinacea* inhibit cyclooxygenase-2 activity in human neuroglioma cells. *Biochem Biophys Res Comm* 2007;360:441–6.
- Gertsch J, Schoop R, Kuenzle U, Suter A. *Echinacea* alkalamides modulate TNF- $\alpha$  gene expression via cannabinoid receptor CB<sub>2</sub> and multiple signal transduction pathways. *FEBS Lett* 2004;577:563–9.
- Raduner S, Majewska A, Chen JZ, Xie XQ, Hamon J, Faller B, et al. Alkylamides from *Echinacea* are a new class of cannabinomimetics. *J Biol Chem* 2006;281:14192–206.
- MacMicking J, Xie QW, Nathan C. Nitric oxide and macrophage function. *Annu Rev Immunol* 1997;15:323–50.
- Maines MD. Heme oxygenase: function, multiplicity, regulatory mechanisms, and clinical application. *FASEB J* 1988;2:2557–68.
- Gabriel KR. The biplot graphical display of matrices with application to principal component analysis. *Biometrika* 1971;58:453–67.
- Gower JC, Hand DJ. *Biplots*. London: Chapman & Hall; 1996.
- Chen CH. Generalized association plots for information visualization: the applications of the convergence of iteratively formed correlation matrices. *Stat Sin* 2002;12:1–23.
- Wu HM, Tien YJ, Chen CH. GAP: a graphical environment for matrix visualization and cluster analysis. *Computational Stat Data Analysis* 2008, in press (doi:10.1016/j.csda.2008.09.029).
- Bauer R, Remiger P, Wagner H. Alkamides from roots of *Echinacea purpurea*. *Phytochemistry* 1988;27:2339–42.
- Chiang YM, Lo CP, Chen YP, Wang SY, Yang NS, Kuo YH, et al. Ethyl caffeate suppresses NF- $\kappa$ B activation and its downstream inflammatory mediators, iNOS, COX-2, and PGE<sub>2</sub> in vitro or in mouse skin. *Br J Pharmacol* 2005;146:352–63.
- Scudiero DA, Shoemaker RH, Paull KD, Monks A, Tierney S, Nofziger TH, et al. Evaluation of a soluble tetrazolium/formazan assay for cell growth and drug sensitivity in culture using human and other tumor cell lines. *Cancer Res* 1988;48:4827–33.
- Lo AH, Liang YC, Lin-Shiau SY, Ho CT, Lin JK. Carnosol, an antioxidant in rosemary, suppresses inducible nitric oxide synthase through down-regulating nuclear factor- $\kappa$ B in mouse macrophages. *Carcinogenesis* 2002;23:983–91.
- Bauer R, Remiger P, Wagner H. Alkamides from roots of *Echinacea angustifolia*. *Phytochemistry* 1989;28:505–8.
- Bauer R, Khan IA, Wray V, Wagner H. Two acetylenic compounds from *Echinacea pallida* roots. *Phytochemistry* 1987;26:1198–200.
- Bauer R, Remiger P, Wray V, Wagner HA. Germacrene alcohol from fresh aerial parts of *Echinacea purpurea*. *Plant Med* 1988;54:478–9.
- Tien YJ, Lee YS, Wu HM, Chen CH. Methods for simultaneously identifying coherent local clusters with smooth global patterns in gene expression profiles. *BMC Bioinformatics* 2008;9:155.
- Hotelling H. Analysis of a complex of statistical variables into principal components. *J Educ Psychol* 1931;24:417–441, 498–520.
- Hotelling H. Simplified calculation of principal components. *Psychometrika* 1936;1:27–35.

- [44] Harman HH. Modern Factor Analysis. Chicago: Univ. of Chicago Press; 1967.
- [45] Malazdrewich C, Thumbikat P, Abrahamsen MS, Maheswaran SK. Pharmacological inhibition of *Mannheimia haemolytica* lipopolysaccharide and leukotoxin-induced cytokine expression in bovine alveolar macrophages. *Microb Pathog* 2004;36:159–69.
- [46] Barrios-Rodiles M, Tiraloché G, Chadee K. Lipopolysaccharide modulates cyclooxygenase-2 transcriptionally and posttranscriptionally in human macrophages independently from Endogenous IL-1 $\beta$  and TNF- $\alpha$ . *J Immunol* 1999;163:963–9.
- [47] Otterbein LE, Bach FH, Alam J, Soares M, Lu HT, Wysk M, et al. Carbon monoxide has anti-inflammatory effects involving the mitogen-activated protein kinase pathway. *Nat Med* 2000;6:422–8.
- [48] Morse D, Pischke SE, Zhou Z, Davis RJ, Flavell RA, Loop T, et al. Suppression of inflammatory cytokine production by carbon monoxide involves the JNK pathway and AP-1. *J Bio Chem* 2003;278:36993–8.
- [49] Oh GS, Pae HO, Choi BM, Chae SC, Lee HS, Ryu DG, et al. 3-Hydroxyanthranilic acid, one of metabolites of tryptophan via indoleamine 2,3-dioxygenase pathway, suppresses inducible nitric oxide synthase expression by enhancing heme oxygenase-1 expression. *Biochem Biophys Res Commun* 2004;320:1156–62.
- [50] Abuarqoub H, Foresti R, Green CJ, Motterlini R. Heme oxygenase-1 mediates the anti-inflammatory actions of 2'-hydroxychalcone in RAW 264.7 murine macrophages. *Am J Physiol Cell Physiol* 2005;290:1092–9.
- [51] Lee SH, Seo GS, Kim JY, Jin XY, Kim HD, Sohn DH. Heme oxygenase-1 mediates anti-inflammatory effects of 2',4',6'-Tris (methoxymethoxy) chalcone. *Eur J Pharmacol* 2006;532:178–86.
- [52] Kang HM, Saltveit ME. Antioxidant capacity of lettuce leaf tissue increases after wounding. *J Agric Food Chem* 2002;50:7536–41.
- [53] Choi YJ, Tomás-Barberán FA, Saltveit ME. Wound-induced phenolic accumulation and browning in lettuce (*Lactuca sativa* L.) leaf tissue is reduced by exposure to *n*-alcohol. *Postharvest Biol Tech* 2005;37:47–55.
- [54] Reyes LF, Cisneros-Zevallos L. Wounding stress increases the phenolic content and antioxidant capacity of purple-flesh potatoes (*Solanum tuberosum* L.). *J Agric Food Chem* 2003;51:5296–300.